Table XI. Measured and Idealized Polyhedral Angles (deg) for $[La(en)_4(trif)]^{2+}$, $[Yb(L)(trif)]^{2+}$, and $[Pr(tren)(trien)(trif)]^{2+}$

face 1	face 2	angle	av angle	idealized angle
	$[La(en)_4(trif)]^{2+}$; D_{3h}			
N5,N6,O1	N2,N4,N8	172.7	172.7	180.0
N1,N2,N5	N3,N6,N8	141.1		146.4
N2,N5,N7	N3,N4,O1	146.1	144.8	146.4
N6,N7,N8	N1,N4,O1	147.3		146.4
N1,N2,N5	N2,N5,N7	21.0		26.4
N6,N7,N8	N3,N6,N8	23.9	25.1	26.4
N3,N4,O1	N1,N4,O1	30.4		26.4
	$[Yb(L)(trif)]^{2+}$; C_{4v}			
N1,N2,N3	N5,N8,O1	161.4	162.2	163.5
N2,N6,O1	N1,N7,N8	162.9		163.5
N1,N3,N7	N5,N6,O1	147.8	142.6	138.2
N2,N3,N6	N5,N7,N8	137.3		138.2
N3,N5,N6	N3,N5,N7	0.6	0.55	0.0
N3,N6,N7	N5,N6,N7	0.5		0.0
	$[Pr(tren)(trien)(trif)]^{2+}$; C_{4v}			
N2,N3,N6	N4,N8,O1	160.4	163.1	163.5
N2,N5,O1	N3,N4,N7	165.7		163.5
N2,N5,N6	N4,N7,N8	145.8	141.9	138.2
N5,N8,O1	N3,N6,N7	138.0		138.2
N5,N6,N7	N5,N7,N8	6.1	6.2	0.0
N6,N7,N8	N5,N6,N8	6.3		0.0

[a] See reference 29.

stabilization to the +3 oxidation states of europium and ytterbium compared to the +2 states. A comparison of the structures of the mono- and dibridged lanthanum complexes implicate the large size of the metal ion as a possible explanation for the difficulty of obtaining and encapsulated complex. However, it is indeed possible to prepare a ytterbium amine complex that is completely encapsulated, and the size of the proposed cage structure is apparently appropriate only for the smallest of the lanthanide ions. Finally, the first example of a mixed amine lanthanide complex has been structurally characterized, but it apparently reacts much slower with the formaldehyde coupling reagent than the bis(tren) complexes do.

Acknowledgment. We acknowledge the late Dr. S. J. Rodgers for helpful discussions and the generous gift of the tren ligand and Dr. F. J. Hollander for his assistance with the structure solutions, which were completed on the CHEXRAY facility (partially supported by the NSF; Grant Nos. CHE-7907027 and CHE-8416692). This work was supported by the Director, Office of Energy Research, Office of Basic Energy Sciences, Chemical Sciences Division of the U.S. Department of Energy, under Contract No. DE-AC03-76SF00098.

Registry No. $Eu(trif)_3$, 52093-25-1; $Yb(trif)_3$, 54761-04-5; $La(tren)_2(trif)_3$, 116840-96-1; $Eu(tren)_2(trif)_3$, 116840-98-3; La(L')$(trif)_3$, 116841-00-0; La(L)$(trif)_3$, 98087-72-0; Yb(L)$(trif)_3$, 98104-54-2; Ce(L)$(trif)_3$, 116841-02-2; Pr(L)$(trif)_3$, 116841-04-4; Eu(L)$(trif)_3$, 116841-06-6; Y(L)$(trif)_3$, 116863-77-5; tren, 4097-89-6; Pr(tren)(trien)$(trif)_3$, 116841-08-8; Yb(L'')$(trif)_3$, 116841-10-2; $Eu(L)^{2+}$, 116841-11-3; $Yb(L)^{2+}$, 116841-12-4; bis(dimethylamino)methane, 51-80-9.

Supplementary Material Available: Figures S-1 and S-2 [disorder models of two of the triflates, S2 and S3, in La(L')$(trif)_3$], Figures S-3 and S-4 [stereoviews of the hydrogen bonding and the unit cell packing diagram for La(L')$(trif)_3$], Figures S-5 and S-6 [stereoviews of the hydrogen bonding and the unit cell packing diagram for Pr(tren)(trien)$(trif)_3$] (7 pages), Tables S-I to S-V [torsion angles, hydrogen bonds, anisotropic thermal parameters, root-mean-square amplitudes of thermal vibration, and calculated hydrogen atom parameters for La(L')$(trif)_3$], and Tables S-VII to S-XI [torsion angles, hydrogen bonds, anisotropic thermal parameters, root-mean-square amplitudes of thermal vibration, and calculated hydrogen atom parameters for Pr(tren)(trien)$(trif)_3$] (20 pages); Tables S-VI and S-XII [F_o and F_c for La(L')$(trif)_3$ and Pr(tren)(trien)$(trif)_3$] (68 pages). Ordering information is given on any current masthead page.

Contribution from the Department of Chemistry, University of Houston, University Park, Houston, Texas 77004

cis- *and trans*-Dioxo Complexes of Chlororuthenium(VI)

S. Perrier and J. K. Kochi*

Received April 19, 1988

Dioxoruthenium(VI) complexes are prepared as the chloro derivatives $O_2RuCl_4^{2-}$ and $O_2RuCl_3^-$ and isolated as the crystalline phosphonium and ammonium salts. Quantitative spectral studies (IR and UV–vis) establish the ready interconversion of the 6-coordinate $O_2RuCl_4^{2-}$ to the 5-coordinate analogue with a dissociation constant $K = 5.3 \times 10^{-3}$ M for chloride loss in dichloromethane. The octahedral structure of $O_2RuCl_4^{2-}$ is established by X-ray crystallography of the $(Ph_3P)_2N^+$ salt to consist of *trans*-dioxo ligands with the asymmetric (A_{2u}) stretching band at 830 cm^{-1} in the IR spectrum. $[(Ph_3P)_2N^+]_2[O_2RuCl_4^{2-}]$: space group $P\bar{1}$ (triclinic) with lattice constants $a = 10.916$ (2) Å, $b = 12.378$ (2) Å, $c = 13.788$ (2) Å, $\alpha = 105.65$ (1)°, $\beta = 93.16$ (1)°, $\gamma = 92.60$ (1)°, and $Z = 1$. The coordinatively unsaturated trichloro derivative $O_2RuCl_3^-$ represents a rare example of a mononuclear dioxo complex whose solid-state structure is dependent on the counterion. Thus, the X-ray crystallography of the $(Ph_3P)_2N^+$ salt establishes a trigonal-bipyramidal structure of $O_2RuCl_3^-$ with the *cis*-dioxo ligands absorbing as a single, strong IR band at 882 cm^{-1}. $[(Ph_3P)_2N^+][O_2RuCl_3^-]$: space group $P2_1/n$ (monoclinic) with lattice constants $a = 10.629$ (4) Å, $b = 15.636$ (5) Å, $c = 21.026$ (7) Å, $\beta = 99.60$ (2)°, and $Z = 4$. The $O_2RuCl_3^-$ ion in the Ph_4P^+ salt is disordered between trigonal-bipyramidal and square-pyramidal geometries, which can be refined by using an occupancy ratio of 6:4 with $R = 0.042$ in the final refinement. The square-pyramidal component of $O_2RuCl_3^-$ is assigned with *trans*-dioxo ligands that account for the appearance of the unusual IR band at 891 cm^{-1} (together with the band at 878 cm^{-1}) in crystalline $[O_2RuCl_3^-][Ph_4P^+]$ [tetragonal space group $P4/n$ with lattice constants $a = 12.672$ (2) Å, $c = 7.788$ (2) Å, and $Z = 2$]. The $(Ph_3P)_2N^+$, Ph_4P^+, Et_4N^+, and n-Bu_4N^+ salts of $O_2RuCl_3^-$ all show a single, sharp IR band at 885 cm^{-1} in solutions of dichloromethane or acetonitrile.

Introduction

Increasing interest accrues for oxometals as viable catalysts for oxygen atom transfer to various substrates.[1,2] Among metal complexes, those of ruthenium are especially attractive since different oxoruthenium species have been identified with the high oxidation states IV–VIII.[3-9] Indeed, the ready availability of such

(1) Holm, R. H. *Chem. Rev.* **1987**, *87*, 1401.
(2) Sheldon, R. A.; Kochi, J. K. *Metal-Catalyzed Oxidation of Organic Compounds*; Academic: New York, 1981.
(3) Seddon, E. A.; Seddon, K. R. *The Chemistry of Ruthenium*; Elsevier: Amsterdam, 1984.
(4) Green, G.; Griffith, W. P.; Hollinshead, D. M.; Ley, S. V.; Schröder, M. *J. Chem. Soc., Perkin Trans. 1* **1984**, 681.

0020-1669/88/1327-4165$01.50/0

multiple oxidation states offers the potential to utilize the ruthenium center (a) to facilitate the reductive elimination of oxo ligands and (b) to promote oxidative addition as in the activation of dioxygen, e.g.

$$Ru^{n} + O_2 \rightleftharpoons \overset{O}{\underset{O}{\diagup\diagdown}}Ru^{n+2} \rightarrow \overset{O}{\underset{O}{\diagup\diagdown}}Ru^{n+4}$$

Oxoruthenium(VIII) and -(VII) are commonly known as ruthenium tetraoxide (RuO_4) and perruthenate (RuO_4^-), no other adducts being structurally characterized or obviously available.[3] Although a number of dioxoruthenium(VI) complexes have been reported,[1,3,10] the structures of only two classes of derivatives have been elucidated by X-ray crystallography, namely the 6-coordinate $O_2Ru^{VI}(tmc)^{2+}$ and $O_2Ru^{VI}(OAc)_2(py)_2$.[7,11] Interestingly, the more substitution-labile chloro derivatives of dioxoruthenium(VI), which are of potential use as synthetic precursors have been observed as the rubidium and cesium salts of 6-coordinate $O_2RuCl_4^{2-}$ as well as the tetraphenylphosphonium salt of 5-coordinate $O_2RuCl_3^-$.[4,12] However, the isolation of two crystalline analogues raises the question of their interconvertibility by chloride ligation, i.e.

$$O_2RuCl_3^- + Cl^- \rightleftharpoons O_2RuCl_4^{2-} \quad (1)$$

It is also important to establish the dispositions of the pair of oxo ligands (i.e., trans or cis) in both the 6-coordinate and the 5-coordinate dioxoruthenium(VI) complexes in eq 1. Accordingly, we report the isolation and spectral characterization of various dioxochlororuthenium(VI) anions, particularly as crystalline salts suitable for X-ray crystallography.

Results and Discussion

Synthesis of Dioxochlororuthenate(VI) Salts. The dark red aqueous solution of 0.1 M ruthenate(VI) was prepared from the alkaline reduction of ruthenium tetraoxide.[13,14] This stock solution was used in the synthesis of the various dioxochlororuthenate(VI) salts as follows.

Dioxotetrachlororuthenate(VI). Addition of 1 equiv of bis(triphenylphosphoranylidene)ammonium (PPN^+) chloride to ruthenate(VI) followed by neutralization of the red solution with hydrochloric acid yielded a green precipitate.[15] Crystallization of the crude mixture from dichloromethane–carbon tetrachloride yielded dark red rhombic crystals of $[(Ph_3P)_2N^+]_2[O_2RuCl_4^{2-}]$ according to the partial stoichiometry in eq 2. Similarly, the

$$RuO_4^{2-} + 2(Ph_3P)_2N^+Cl^- \xrightarrow{HCl} [(Ph_3P)_2N^+]_2[O_2RuCl_4^{2-}] + H_2O \quad (2)$$

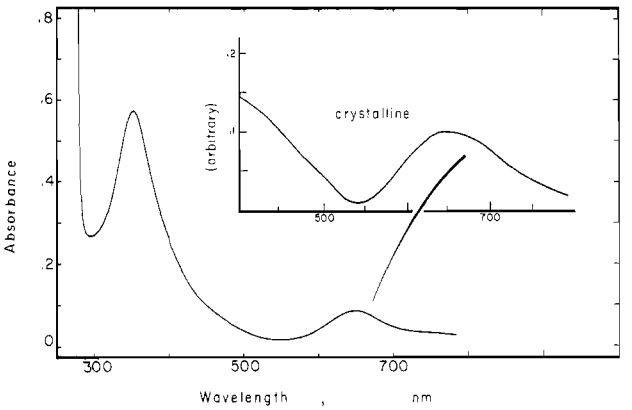

Figure 1. Electronic spectrum of $O_2RuCl_3^-$ from a 2×10^{-4} M solution of the Ph_4P^+ salt in dichloromethane. The diffuse-reflectance spectra of crystalline $[Ph_4P^+][O_2RuCl_3^-]$ diluted with powdered silica gel is shown in the inset.

phosphonium salt $[Ph_4P^+]_2[O_2RuCl_4^{2-}]$ was prepared as dark red crystals by the neutralization of the ruthenate(VI) solution containing excess tetraphenylphosphonium chloride with hydrochloric acid.

Dioxotrichlororuthenate(VI). Addition of 1 equiv of tetraphenylphosphonium chloride to the stock solution of 0.1 M ruthenate(VI) followed by neutralization with hydrochloric acid yielded a green precipitate. Crystallization from a mixture of dichloromethane and carbon tetrachloride led to emerald green rodlike crystals of $[Ph_4P^+][O_2RuCl_3^-]$. The corresponding PPN^+ salt was prepared by the treatment of $[(Ph_3P)_2N^+]_2[O_2RuCl_4^{2-}]$ with 1 equiv of silver tetrafluoroborate in acetonitrile solution to afford immediately a precipitate of silver chloride, which was separated by filtration. Removal of the solvent in vacuo, followed by crystallization of the green solid, led to $[(Ph_3P)_2N^+][O_2RuCl_3^-]$ as emerald green diamond-shaped crystals. The tetraethylammonium and tetra-*n*-butylammonium salts of $O_2RuCl_3^-$ were prepared by Howe's procedure for the alkali-metal salts.[12] The thin emerald green flakes could not be successfully recrystallized in forms suitable for X-ray crystallography (see Experimental Section).

Spectroscopic Properties of Dioxochlororuthenate(VI) Salts. Infrared spectra of oxometal complexes are generally characterized by the presence of characteristic absorption bands between ~800 and 1050 cm^{-1}.[16,17] The stretching frequencies of the dioxometals are usually concentrated in the lower end of this spectral range, namely between 800 and 900 cm^{-1}.[17,18] In accord with these generalizations, the IR absorptions of 6-coordinate $O_2RuCl_4^{2-}$ in the solid state (KBr) occurred as single, sharp bands at 828 and 834 cm^{-1} for the $(Ph_3P)_2N^+$ and Ph_4P^+ salts, respectively. Interestingly, the location of the bands was consistent with those found at 840 ± 20 cm^{-1} in other 6-coordinate dioxoruthenium(VI) derivatives with the *trans*-dioxoruthenium configuration, irrespective of the overall charge on the complex.[5,6e,7] It is particularly noteworthy that the O=Ru stretching bands of the 6-coordinate salts $[(Ph_3P)_2N^+]_2[O_2RuCl_4^{2-}]$ and $[Ph_4P^+]_2[O_2RuCl_4^{2-}]$ were both shifted to significantly higher energy (885 cm^{-1}) when they were dissolved in either dichloromethane or acetonitrile. The new IR spectrum corresponded to that of the 5-coordinate $O_2RuCl_3^-$ salts. For example, the $(Ph_3P)_2N^+$, Et_4N^+, and n-Bu_4N^+ salts of $O_2RuCl_3^-$ in the solid state (KBr) showed a single, sharp absorption band at 881, 881, and 884 cm^{-1}, respectively. Since the same band (885 cm^{-1}) persisted in solution, the foregoing spectral shift was diagnostic of the clean conversion of 6-coordinate $O_2RuCl_4^{2-}$ to 5-coordinate $O_2RuCl_3^-$ upon dissolution in either dichloromethane or acetonitrile solutions according to eq 1.

(5) (a) Groves, J. T.; Quinn, R. *J. Am. Chem. Soc.* **1985**, *107*, 5790. (b) Groves, J. T.; Ahn, K. Y. *Inorg. Chem.* **1987**, *26*, 2831.
(6) (a) Che, C.-M.; Wong, K.-Y.; Poon, C.-K. *Inorg. Chem.* **1985**, *24*, 1797. (b) Che, C.-M.; Wong, K.-Y.; Leung, W.-H.; Poon, C.-K. *Inorg. Chem.* **1986**, *25*, 345. (c) Che, C.-M.; Wong, K.-Y. *J. Chem. Soc., Chem. Commun.* **1986**, 229. (d) Mak, T. C. W.; Che, C.-M.; Wong, K.-Y. *J. Chem. Soc., Chem. Commun.* **1985**, 986. (e) Che, C.-M.; Lai, T.-F.; Wong, K.-Y. *Inorg. Chem.* **1987**, *26*, 2289.
(7) Lau, T. C.; Kochi, J. K. *J. Chem. Soc., Chem. Commun.* **1987**, 798.
(8) Griffith, W. P.; Ley, S. V.; Whitecombe, G. P.; White, A. D. *J. Chem. Soc., Chem. Commun.* **1987**, 1625.
(9) (a) Gulliver, D. J.; Levason, W. *Coord. Chem. Rev.* **1982**, *46*, 1. (b) Stravropoulos, P.; Edwards, P. G.; Behling, T.; Wilkinson, G.; Motevalli, M.; Hursthouse, M. B. *J. Chem. Soc., Dalton Trans.* **1987**, 169. (c) Takeuchi, K. J.; Samuels, G. J.; Gersten, S. W.; Gilbert, J. A.; Meyer, T. J. *Inorg. Chem.* **1983**, *22*, 1407. (d) Bailey, C. L.; Drago, R. S. *J. Chem. Soc., Chem. Commun.* **1987**, 179. (e) Collin, J. D.; Sauvage, J. P. *Inorg. Chem.* **1986**, *25*, 135. (f) Che, C.-M.; Leung, W.-H. *J. Chem. Soc., Chem. Commun.* **1987**, 1376.
(10) Griffith, W. P. *The Chemistry of the Rarer Platinum Metals* (Os, Ru, Ir and Rh); Wiley-Interscience: New York, 1967.
(11) tmc (=tetramethyltetraazacyclotetradecane) and analogues as described by Che et al. in ref 6e.
(12) (a) Howe, J. L. *J. Am. Chem. Soc.* **1901**, *23*, 775. (b) See also: Hepworth, M. A.; Robinson, P. L. *J. Inorg. Nucl. Chem.* **1957**, *4*, 24.
(13) Beynon, P. J.; Collins, D.; Gardiner, D.; Overend, W. G. *Carbohydr. Res.* **1968**, *6*, 431.
(14) (a) Mijs, W. J.; De Jonge, C. R. H. J. *Organic Syntheses by Oxidation with Metal Compounds*; Plenum: New York, 1986. (b) See also ref 4.
(15) This solid is actually an equimolar mixture of $[PPN^+][O_2RuCl_3^-]$ and $[PPN^+][Cl^-]$.
(16) Griffith, W. P. *J. Chem. Soc. A* **1969**, 211.
(17) (a) Jezowska-Trzebiatowska, B.; Hanuza, J.; Baluka, M. *Acta Phys. Pol.* **1970**, *A38*, 563. (b) Schmidt, K. H.; Müller, A. *Coord. Chem. Rev.* **1974**, *14*, 115.
(18) Griffith, W. P.; Wickins, T. D. *J. Chem. Soc. A* **1968**, 400.

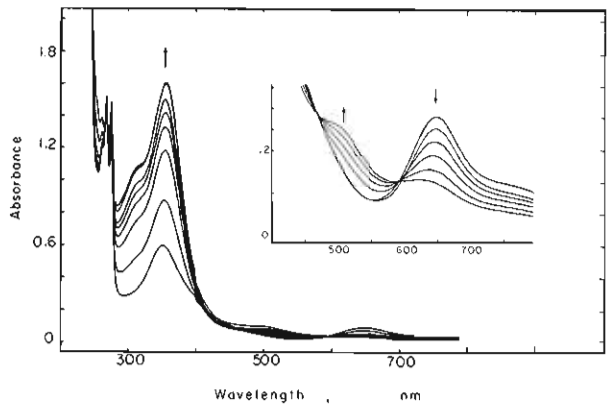

Figure 2. Effect of incremental additions of (bottom to top) 0, 4, 8, 12, 16, 20, 30, and 40 equiv of $[Et_4N^+][Cl^-]$ to a 2×10^{-4} M solution of $[Ph_4P^+][O_2RuCl_3^-]$ in dichloromethane. Inset is the absorbance enlargement of the 450–750-nm region, showing the pair of isosbestic points.

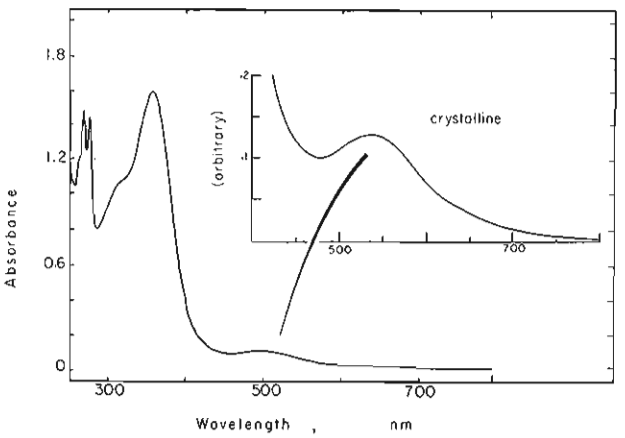

Figure 3. Electronic spectrum of $O_2RuCl_4^{2-}$ from 2×10^{-4} M $[Ph_4P^+][O_2RuCl_3^-]$ in dichloromethane containing 40 equiv of $[Et_4N^+][Cl^-]$. The inset shows the diffuse-reflectance spectrum of crystalline $[(Ph_3P)_2N^+]_2[O_2RuCl_4^{2-}]$ diluted with powdered silica gel.

However the situation was not quite so clear-cut in the solid-state (KBr) spectrum of the Ph_4P^+ salt of $O_2RuCl_3^-$, which exhibited a *pair* of IR stretching bands at 891 and 878 cm^{-1}, as previously described by Griffith.[4] The latter (878 cm^{-1}) was within the spectral resolution (±2 cm^{-1}) the same as those of the ammonium salts (vide supra). However, the second band at 891 cm^{-1} clearly occurred at an anomalously high energy for it to be considered in the same way. Moreover, it was significant that the twin bands merged into a single band at 885 cm^{-1} when $[Ph_4P^+][O_2RuCl_3^-]$ was dissolved in either dichloromethane or acetonitrile.

The electronic spectrum of $O_2RuCl_3^-$ in Figure 1 (commonly obtained from the dissolution of the various ammonium and phosphonium salts in dichloromethane or acetonitrile) is characterized by a strong absorption band at 353 nm (ϵ 2820 M^{-1} cm^{-1}) and a weak absorbance at 648 nm (ϵ 470 M^{-1} cm^{-1}). The latter is responsible for the emerald green color of the 5-coordinate dioxotrichlororuthenate(VI) complex, as shown by comparison with the diffuse reflectance spectrum of the crystalline $[Ph_4P^+][O_2RuCl_3^-]$ presented in the inset of Figure 1. It is noteworthy that the solution spectrum in Figure 1 was also obtained when 6-coordinate $O_2RuCl_4^{2-}$, either as the $(Ph_3P)_2N^+$ or Ph_4P^+ salt, was dissolved in dichloromethane and acetonitrile. Since the latter suggested a mobile equilibrium for the anation in eq 1, the spectral dependence on added chloride was examined separately.

Reversible Interconversion of 5- and 6-Coordinate Dioxochlororuthenium(VI). The successive addition of chloride (as the tetraethylammonium salt) to a solution of 5-coordinate $O_2RuCl_3^-$ led to a striking change in the green solution to orange. The series of spectra resulting from the incremental addition of chloride to 2×10^{-4} M $O_2RuCl_3^-$ is shown in Figure 2 as the disappearance of the absorption centered at λ_{max} 648 nm and the appearance of a new band at ~500 nm. The presence of a pair of isosbestic points at 592 and 470 nm (see inset, Figure 2) was associated with the formation of 6-coordinate $O_2RuCl_4^{2-}$. The latter was established by the comparison of the limiting spectrum in Figure 3 obtained from 2×10^{-4} M $O_2RuCl_3^-$ at the high chloride concentrations of $[[Et_4N^+][Cl^-]] > 10^{-2}$ M with the diffuse-reflectance spectrum of the crystalline $[(Ph_3P)_2N^+]_2[O_2RuCl_4^{2-}]$ shown in the inset.

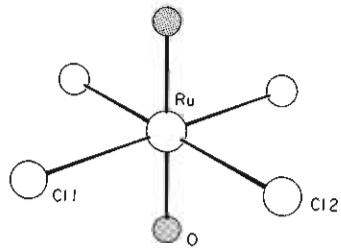

Figure 4. Diagram of the *trans*-dioxo ligands in the octahedral $O_2RuCl_4^{2-}$ in the $(Ph_3P)_2N^+$ salt.

Table I. Bond Lengths (Å) in Dioxochlororuthenium(VI) Complexes

	A. $[(Ph_3P)_2N^+]_2[O_2RuCl_4^{2-}]$		
Ru–Cl(1)	2.388 (2)	Ru–Cl(2)	2.394 (2)
Ru–O	1.709 (4)		
	B. $[(Ph_3P)_2N^+][O_2RuCl_3^-]$		
Ru–Cl(1)	2.374 (6)	Ru–Cl(2)	2.390 (6)
Ru–Cl(3)	2.133 (4)	Ru–O(1)	1.658 (5)
Ru–O(2)	1.694 (9)	Ru′–Cl(1′)	2.346 (6)
Ru′–Cl(2′)	2.338 (7)	Ru′–Cl(3′)	2.177 (5)
Ru′–O(1)	1.713 (5)	Ru′–O(2′)	1.768 (8)
Ru–Ru′	0.073 (2)		
	C. $[Ph_4P^+][O_2RuCl_3^-]$		
Ru–Cl	2.367 (2)	Ru–O(1)	1.785 (32)
Ru–O(1′)	1.595 (21)	Ru–O(2)	1.649 (25)
Ru–O(2′)	1.643 (25)		

The dissociation constant K for eq 1 was determined spectrophotometrically by measuring the disappearance of $O_2RuCl_3^-$ by its absorbance decrease at λ_{max} 648 nm that was attendant upon the incremental addition of tetraethylammonium chloride. The magnitude of $K = 5.3 \times 10^{-3}$ M established in dichloromethane (see Experimental Section) was sufficient to predict the complete dissociation of 6-coordinate $O_2RuCl_4^{2-}$ in 10^{-3} M salt solutions (eq 1). This result thus provides a complete explanation of the spectral (IR, UV–vis) behavior of the crystalline salts of $O_2RuCl_4^{2-}$ relative to those in solution.

Molecular Structures of 5- and 6-Coordinate Dioxochlororuthenium(VI). Although the salts of dioxochlororuthenium(VI) have been known since the turn of the century,[12] none of their structures have been established by X-ray crystallography. For 6-coordinate $O_2RuCl_4^{2-}$, an octahedral structure with either a cis or trans configuration of the dioxo ligands is possible,[17] viz.

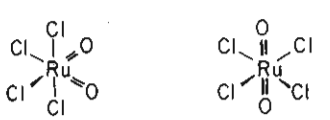

For example, such 6-coordinate dioxometal complexes as $O_2WCl_4^{2-}$, $O_2MoCl_4^{2-}$, and $O_2VF_4^{3-}$ have been assigned the *cis*-dioxo structure.[18] On the other hand, X-ray studies have established the dioxometalates $O_2Mo(CN)_4^{4-}$, $O_2OsCl_4^{2-}$, and $O_2Re(CN)_4^{3-}$ to have the *trans*-dioxo structure.[16,17]

X-ray crystallography of the dark red rhombic crystal of $[(Ph_3P)_2N^+]_2[O_2RuCl_4^{2-}]$ established the *trans*-dioxo structure, as illustrated in the diagram in Figure 4. The linear arrangement of *trans*-O=Ru=O is thus the same as that observed in the cationic $O_2Ru(tmc)^+$ and the uncharged $O_2Ru(O_2CCH_3)_2(py)_2$.[7,11] Indeed, the O=Ru bond distance of 1.71 Å in $O_2RuCl_4^{2-}$ (Table I) compares with 1.70 Å in $O_2Ru(tmc)^+$ and 1.73 Å in O_2Ru-

Table II. Bond Angles (deg) in Dioxochlororuthenium(VI) Complexes

	A. $[(Ph_3P)_2N^+]_2[O_2RuCl_4^{2-}]$		
Cl(2)–Ru–Cl(1)	90.3 (1)	O–Ru–Cl(1)	88.7 (1)
O–Ru–Cl(2)	89.2 (1)	Cl(1)–Ru–Cl(2′)	89.7 (1)
Cl(1)–Ru–O′	91.3 (1)	Cl(2)–Ru–O′	90.8 (1)
	B. $[(Ph_3P)_2N^+][O_2RuCl_3^-]$		
Cl(2)–Ru–Cl(1)	174.5 (3)	Cl(3)–Ru–Cl(1)	94.5 (3)
Cl(3)–Ru–Cl(2)	90.3 (2)	O(1)–Ru–Cl(1)	88.9 (3)
O(1)–Ru–Cl(2)	87.0 (3)	O(1)–Ru–Cl(3)	110.8 (2)
O(2)–Ru–Cl(1)	91.7 (7)	O(2)–Ru–Cl(2)	87.9 (7)
O(2)–Ru–Cl(3)	121.9 (6)	O(2)–Ru–O(1)	127.1 (6)
Cl(2′)–Ru′–Cl(1′)	175.7 (3)	Cl(3′)–Ru′–Cl(1′)	88.6 (3)
Cl(3′)–Ru′–Cl(2′)	94.3 (4)	O(1)–Ru′–Cl(1′)	88.7 (3)
O(1)–Ru′–Cl(2′)	93.0 (3)	O(1)–Ru′–Cl(3′)	114.1 (3)
O(2′)–Ru′–Cl(1′)	87.6 (4)	O(2′)–Ru′–Cl(2′)	88.4 (4)
O(2′)–Ru′–Cl(3′)	110.9 (4)	O(2′)–Ru′–O(1)	137.7 (4)
	C. $[Ph_4P^+][O_2RuCl_3^-]$		
Cl–Ru–Cl′	89.9 (1)	Cl–Ru–Cl″	89.9 (1)
Cl′–Ru–Cl″	174.5 (1)	O(1)–Ru–Cl	92.7 (1)
O(1)–Ru–Cl′	92.7 (1)	O(1)–Ru–Cl″	92.7 (1)
O(1′)–Ru–Cl	112.4 (10)	O(1′)–Ru–Cl′	92.7 (10)
O(1′)–Ru–Cl′	92.5 (10)	O(1′)–Ru–O(1)	19.6 (10)
O(2)–Ru–Cl	87.3 (1)	O(2)–Ru–Cl′	87.3 (1)
O(2)–Ru–Cl″	87.3 (1)	O(2)–Ru–O(1)	180.0
O(2′)–Ru–Cl	121.3 (8)	O(2′)–Ru–Cl′	87.9 (8)
O(2′)–Ru–Cl″	87.6 (8)	O(2′)–Ru–O(1′)	126.3 (12)
O(2′)–Ru–O(2)	34.0 (8)		

$(O_2CCH_3)_2(py)_2$. The bond angles for O–Ru–Cl and Cl–Ru–Cl in Table II accord with the centrosymmetric structure of D_{4h} symmetry shown in Figure 4. Accordingly, the O=Ru stretching frequency of 830 cm^{-1} in the IR spectrum of $O_2RuCl_4^{2-}$ represents the asymmetric A_{2u} mode. As such, it is well within the range of IR frequencies (760–840 cm^{-1}) observed with a variety of other *trans*-dioxometal complexes of the general type O_2MX_4 and $O_2MX_2Y_2$.[16,17] These characteristic (single) absorption bands compare with the appearance of a pair of IR-active bands at ~950 and ~900 cm^{-1} that correspond to the symmetric (A_{1g}) and asymmetric (B_1) stretching modes of *cis*-dioxometal complexes with C_{2v} symmetry.[18]

For 5-coordinate $O_2RuCl_3^-$, a trigonal-bipyramidal (tbp) or square-pyramidal (sp) configuration is possible with either *cis*- or *trans*-dioxo ligand arrangement,[19] e.g.

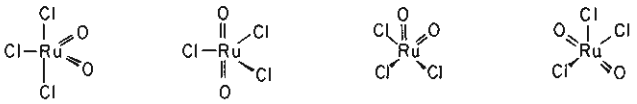

However, such idealized tbp structures are rarely found in practice, and experimental differences are usually subtle, since only a slight deformation is sufficient to convert one such structure into the other. The difficulty has been underscored by Rossi and Hoffmann,[20] who describe the separation of the energy minima of tbp from sp by a soft potential energy surface. The few crystallographic analyses of dioxometal complexes of the general composition O_2MX_3 such as $O_2VF_3^{2-}$ and $O_2MoF_3^-$ have shown them to consist of associated octahedral units with bridging (fluoride) ligands.[21] Recent examples of distorted tbp structures of d^0 *cis*-dioxo complexes include the sterically encumbered analogues $O_2Mo(mesityl)_2CH_2PBu_3$, $O_2W(OCMe_2CMe_2O)(CH_2CMe_3)^-$, and $O_2Re(CH_2CMe_3)_3$.[22] Otherwise, the structural assignments

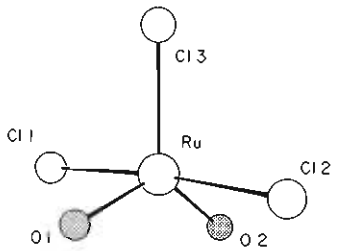

Figure 5. Diagram of the *cis*-dioxo ligands in the trigonal-bipyramidal $O_2RuCl_3^-$ in the $(Ph_3P)_2N^+$ salt.

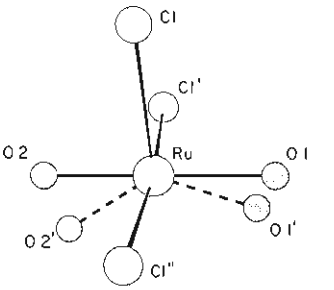

Figure 6. Diagram of the disordered $O_2RuCl_3^-$ anion in the Ph_4P^+ salt analyzed as the superposition of the trigonal-bipyramidal (O(1′), O(2′)) and square-pyramidal (O(1), O(2)) occupancies as described in the text.

of various 5-coordinate dioxometal complexes such as O_2ReF_3, $O_2Re(CH_3)_3$, $O_2CrF_3^-$, $O_2UCl_3^-$, and O_2OsF_3 have been based on spectral (sporting) methods.[19,23-28] Unfortunately, an unambiguous structural assignment based on vibrational analysis of 5-coordinate $O_2RuCl_3^-$ is obscured by the different sets of IR bands in solid-state IR spectra of the $(Ph_3P)_2N^+$ and Ph_4P^+ salts (vide supra). Our X-ray crystallographic analysis of $O_2RuCl_3^-$ was beset by the ubiquitous crystalline disorder encountered with both salts despite numerous attempts to grow quality crystals in various solvents and under different conditions (see Experimental Section). Nonetheless we succeeded in growing a single crystal of $[(Ph_3P)_2N^+][O_2RuCl_3^-]$, in which the disorder merely consisted of two slightly different tbp orientations of the anionic $O_2RuCl_3^-$, the structure of the cationic $(Ph_3P)_2N^+$ moiety being highly refined. The diagram in Figure 5 shows one of the mononuclear tbp units of $O_2RuCl_3^-$, in which the pair of oxo ligands lie in the equatorial plane with a O=Ru=O angle of 127°. This internal angle is slightly wider than that found for the equatorial trioxo ligands in the trigonal-bipyramidal ruthenate(VI) $O_3Ru(OH)_2^{2-}$.[29] The apical → apical bond angle of 175° for Cl–Ru–Cl is slightly distorted from linearity, but it is bisected by the equatorial chloro–dioxo plane to adequately describe the overall tbp configuration.[30] The structure of trigonal-bipyramidal $O_2RuCl_3^-$

(19) Beattie, I. R.; Crocombe, R. A.; Ogden, J. S. *J. Chem. Soc., Dalton Trans.* **1977**, 1481. See also: Glukhov, I. A.; El'manova, N. A.; Eliseev, S. S.; Temurova, M. T. *Russ. J. Inorg. Chem. (Engl. Transl.)* **1974**, *19*, 168.

(20) Rossi, A. R.; Hoffmann, R. *Inorg. Chem.* **1975**, *14*, 365. For a review of 5-coordinate structures, see: Holmes, R. R. *Prog. Inorg. Chem.* **1984**, *32*, 119.

(21) (a) Ryan, R. R.; Mastin, S. H.; Reisfeld, M. J. *Acta Crystallogr.* **1971**, *B27*, 1270. (b) Atovmyan, L. O.; Krasochka, O. N.; Rahlin, M. Ya. *J. Chem. Soc., Chem. Commun.* **1971**, 610. (c) Mattes, R.; Müller, G.; Becher, H. J. *Z. Anorg. Allg. Chem.* **1972**, *389*, 177.

(22) (a) Lai, R.; Le Bot, S.; Baldy, A.; Pierrot, M.; Arzoumanian, H. *J. Chem. Soc., Chem. Commun.* **1986**, 1208. (b) Feinstein-Jaffe, I.; Dewan, J. C.; Schrock, R. *Organometallics* **1985**, *4*, 1189. (c) Cai, S.; Hoffman, D. M.; Wierda, D. A. *J. Chem. Soc., Chem. Commun.* **1988**, 313.

(23) (a) Mertis, K.; Wilkinson, G. *J. Chem. Soc., Dalton Trans.* **1976**, 1488. See also: Cai, S.; Hoffman, D. M.; Lappas, D.; Woo, H. G. *Organometallics* **1987**, *6*, 2273. (b) Green, P. J.; Gard, G. L. *Inorg. Nucl. Chem. Lett.* **1978**, *14*, 179.

(24) Bagnall, K. W.; du Preez, J. G. H.; Gellatly, B. J.; Holloway, J. H. *J. Chem. Soc., Dalton Trans.* **1975**, 1963.

(25) Falconer, W. E.; Disalvo, F. J.; Griffiths, J. E.; Stevie, F. A.; Sunder, W. A.; Vasile, M. J. *J. Fluorine Chem.* **1975**, *6*, 499.

(26) Pausewang, G.; Dehnicke, K. *Z. Anorg. Allg. Chem.* **1969**, *369*, 265.

(27) Franklin, K. J.; Lock, C. J. L.; Sayer, B. G.; Schrobilgen, G. J. *J. Am. Chem. Soc.* **1982**, *104*, 5303.

(28) See also: (a) Buslaev, Yu. A.; Davidovich, R. L. *Russ. J. Inorg. Chem. (Engl. Transl.)* **1968**, *13*, 656. (b) Beiles, R. G.; Samorodova, V. S.; Rozmanova, Z. E. *Russ. J. Inorg. Chem. (Engl. Transl.)* **1973**, *18*, 1583. (c) Davidovich, R. L.; Buslaev, Yu. A.; Sergienko, V. I.; Ivanov, S. G.; Peshkov, V. V.; Mikhailov, Yu. N. *Dokl. Akad. Nauk SSSR* **1974**, *219*, 332.

(29) (a) Nowogrocki, G.; Abraham, F.; Trêhoux, J.; Thomas, D. *Acta Crystallogr., Sect. B* **1976**, *32*, 2413. (b) Elout, M. O.; Haije, W. G.; Maaskant, W. J. A. *Inorg. Chem.* **1988**, *27*, 610.

in Figure 5 together with the electronic spectra in Figure 1 thus establishes the assignment of the IR band at 881 ± 3 cm^{-1} specifically to the asymmetric stretching mode of the *cis*-dioxo ligands.[31] both in the solid state and in solution.

Such an unequivocal vibrational assignment of the *cis*-dioxo ligands now raises the question as to the structure of the $O_2RuCl_3^-$ moiety extent in the crystalline Ph_4P^+ salt that exhibits a pair of IR bands at 891 and 878 cm^{-1}. In order to answer this question, we made repeated attempts to grow single crystals of $[Ph_4P^+][O_2RuCl_3^-]$ suitable for X-ray crystallography. After numerous trials, out best effort yielded an emerald green crystal in which the phosphonium cation was highly ordered but the $O_2RuCl_3^-$ moiety suffered some disorder. The structure of $[Ph_4P^+][O_2RuCl_3^-]$ was solved by the use of the Patterson interpretation program,[33] which revealed the position of the Ru atom in an asymmetric unit with $O_2RuCl_3^-$ and $(Ph_3P)_2N^+$ lying on a 4-fold axis and $\bar{4}$ symmetry site, respectively. The best model we could develop from the disordered anion (see Experimental Section) was based on a 6:4 occupancy of tbp:sp structures. The trigonal-bipyramidal component was that in Figure 5 derived from the $(Ph_3P)_2N^+$ salt. The other component was based on the square-pyramidal configuration that was previously developed from the X-ray crystallography of the ruthenium(VI) salt $[Ph_4As^+][RuNCl_4^-]$.[34] The juxtaposition of the tbp and sp forms of $O_2RuCl_3^-$ is presented in Figure 6. The essential correctness of this model is given in the final refinement by $R = 0.042$ ($R_w = 0.024$) with insignificant residual electron density above the background.[35] If so, it clarifies the hitherto puzzling presence of two dioxo bands in the solid-state IR spectrum of $[Ph_4P^+][O_2RuCl_3^-]$. Thus, the low-energy band at 878 cm^{-1} is clearly within experimental uncertainty the same as that observed for the trigonal-bipyramidal $O_2RuCl_3^-$ moiety in the crystalline $(Ph_3P)_2N^+$ salt. By the same reasoning, the higher energy band at 891 cm^{-1} is then assigned to the *trans*-dioxo ligands in the 5-coordinate square-pyramidal configuration. The minor distortions in Figure 6 reemphasize the gross similarities of these tbp and sp structures in the solid state, the distinction between which obviously disappears entirely upon the dissolution of the $(Ph_3P)_2N^+$ and Ph_4P^+ salts.

Oxygen Atom Transfer from Dioxochlororuthenium(VI). Having described the dynamic properties of the various dioxochlororuthenium(VI) complexes, we also briefly examined their ability to effect oxygen atom transfer to three representative substrates—phosphine, alkene, and phenol. At this juncture, we present only preliminary studies of the nature of oxidation products owing to the difficulty of isolating the reduced ruthenium species in pure crystalline form.

When an acetonitrile solution of 0.2 M $[Ph_4P^+][O_2RuCl_3^-]$ was treated with 1 equiv of triphenylphosphine, a quantitative yield of triphenylphosphine oxide was obtained according to the (apparent) stoichiometry

$$O_2RuCl_3^- + PPh_3 \rightarrow OPPh_3 + ORuCl_3^- \qquad (3)$$

A similar oxidation of dimethylphenylphosphine occurred readily, as judged by the disappearance of the diagnostic IR band at 885 cm^{-1} within 1 h. Free dimethylphenylphosphine oxide was not detected by gas chromatographic analysis. This phosphine oxide was undoubtedly still bound to the reduced ruthenium product, as deduced from the liberation of $OPPhMe_2$ upon the addition of excess pyridine to the crude reaction mixture that also showed the characteristic IR band at 1131 cm^{-1} for the coordinated ligand.[36]

The treatment of an emerald green solution of 0.2 M $[Ph_4P^+][O_2RuCl_3^-]$ in acetonitrile with 1 equiv of cyclohexene caused progressive darkening over a 2-h period.[38] Analysis of the reaction mixture by GC–MS indicated a complex mixture of products that included cyclohexene oxide, 2-cyclohexenone, 2-chlorocyclohexanone, and cyclohexene chlorohydrin in more or less equimolar amounts (see Experimental Section). The same oxidation carried out in dichloromethane afforded more 2-chlorocyclohexanone at the expense of cyclohexene oxide. On the basis of these products, we tentatively suggest that oxygen atom transfer from $O_2RuCl_3^-$ yields two primary products,[39] i.e.

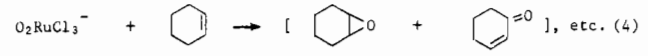

followed by further oxidation.

The oxidation of the hindered phenol 2,6-di-*tert*-butylphenol with 0.2 M $[Ph_4P^+][O_2RuCl_3^-]$ in acetonitrile occurred upon mixing, as indicated by instantaneous color change of the solution to green black. GC–MS analysis of the reaction mixture established the formation of 2,6-di-*tert*-butyl-*p*-benzoquinone, i.e.

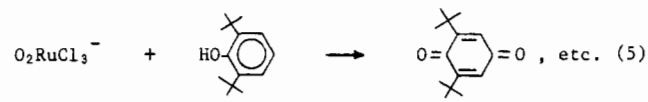

In addition, the binuclear 3,5,3′,5′-tetra-*tert*-butyldiphenoquinone from the oxidative coupling of the phenol was also observed.[40]

The complexion of the oxidation products derived from the phosphines and cyclohexene in eq 3 and 4 suggests that dioxotrichlororuthenate(VI) is indeed capable of oxygen atom transfer to relatively electron-rich substrates. Moreover, the formation of the coupled diphenoquinone in addition to the quinone in eq 5 is also indicative of a stepwise process involving phenoxy radicals as reactive intermediates.[41] If so, multiple pathways for the reduction of dioxoruthenium(VI) may exist to afford a common series of oxoruthenium species, as qualitatively judged by the same green-black solution obtained finally from the structurally quite dissimilar substrates described by eq 3–5.

Experimental Section

Materials. Ruthenium(III) chloride, $RuCl_3 \cdot 3H_2O$ (Platina Laboratories), bis(triphenylphosphoranylidene)ammonium chloride and tetraphenylphosphonium chloride (Aldrich), sodium periodate (Mallinckrodt), and silver tetrafluoroborate (Aldrich) were used as received. Tetraethylammonium chloride (Aldrich) was dried azeotropically from benzene and stored under argon. Cyclohexene (Mallinckrodt) was distilled from lithium aluminum hydride and stored under argon. Triphenylphosphine (Aldrich) was recrystallized from *n*-hexane, and dimethylphenylphosphine (Aldrich) was distilled from sodium, and both were stored under an argon atmosphere. 2,6-Di-*tert*-butylphenol (Aldrich) was recrystallized from hexane. Dichloromethane (Baker) was repeatedly stirred with fresh concentrated sulfuric acid until the acid layer remained colorless. It was washed with water and aqueous sodium bicarbonate and dried with calcium chloride. It was initially distilled from phosphorus pentoxide and then redistilled from calcium hydride under an argon atmosphere. Acetonitrile (Mallinckrodt reagent grade) was stirred over potassium permanganate for 24 h, filtered, and distilled. The distillate was refluxed over phosphorus pentoxide and then distilled under an argon atmosphere. It was redistilled from calcium hydride. *n*-Hexane and benzene (Mallinckrodt) were stirred over fresh concentrated sulfuric acid

(30) The C_{2v} symmetry in a d^2 ruthenium(VI) complex with *cis*-dioxo ligands should lead to a triplet ground state (Albright, T. A., private communication). The diamagnetism of $[Ph_4P^+][O_2RuCl_3^-]$ (see Experimental Section) is similar to that found in 6-coordinate *cis*-$O_2Os(bpy)_2^{2+}$, and it may be due to the lowering of the symmetry as a result of the enlarged O=Ru=O angle of 127°. [Compare: Dobson, J. C.; Takeuchi, K. J.; Pipes, D. W.; Geselowitz, D. A.; Meyer, T. J. *Inorg. Chem.* **1986**, *25*, 2357.] See also: Ciani, J.; D'Alfonso, G.; Romiti, P. F.; Sironi, A.; Freni, M. *Inorg. Chim. Acta* **1985**, *72*, 29.

(31) Compare with the band at 879 cm^{-1} in the IR spectrum of the analogous *cis*-dioxoosmium(VI) complex examined earlier.[32] The symmetric stretch at 919 cm^{-1} is weak.

(32) Cartwright, B. A.; Griffith, W. P.; Schröder, M.; Skapski, A. C. *J. Chem. Soc., Chem. Commun.* **1978**, 853.

(33) Sheldrick, G. M. *SHELXTL PLUS Programs for Crystal Structure Determination*; Nicolet XRD Corp.: Madison, WI, 1987.

(34) Philipps, F. L.; Skapski, A. C. *Acta Crystallogr., Sect. B* **1975**, *31*, 2667.

(35) See Experimental Section for a detailed description of this point.

(36) If P=O stretching band in Ph_3PO at 1185 cm^{-1} generally decreases by 50 cm^{-1} on metal coordination.[37]

(37) Nakamoto, K. *Infrared Spectra of Inorganic and Coordination Compounds*, 2nd ed.; Wiley: New York, 1970.

(38) Experiments performed by T. C. Lau (1986).

(39) Compare: (a) Srinivasan, K.; Perrier, S.; Kochi, J. K. *J. Mol. Catal.* **1986**, *36*, 297. (b) Koola, J. D.; Kochi, J. K. *J. Org. Chem.* **1987**, *52*, 4545.

(40) See: Kharasch, M. S.; Joshi, B. S. *J. Org. Chem.* **1957**, *22*, 1439.

(41) Compare: Tada, M.; Katsu, T. *Bull. Chem. Soc. Jpn.* **1972**, *45*, 2558.

until the acid layer remained colorless and they were then washed with water and aqueous sodium bicarbonate. They were dried over calcium chloride and then distilled from sodium under an argon atmosphere. Diethyl ether (Baker, anhydrous) was distilled from sodium benzophenone under an argon atmosphere.

Ruthenium(III) chloride was converted to ruthenium dioxide, $RuO_2 \cdot 2H_2O$, according to Beynon's procedure,[13] $RuO_2 \cdot 2H_2O$ (0.2 g, 1.2 mmol) suspended in water was oxidized with sodium periodate (0.75 g, 3.5 mmol), and the ruthenium tetraoxide was extracted into carbon tetrachloride.[4] The solution of RuO_4 in CCl_4 was shaken with concentrated potassium hydroxide to yield a dark red solution of ~0.1 M ruthenate(VI) RuO_4^{2-}, which was always used in all subsequent preparations.

$[Ph_4P^+]_2[O_2RuCl_4^{2-}]$. The ruthenate solution (from 1.2 mmol of RuO_2) was cooled in an ice bath, and a saturated solution of $[Ph_4P^+][Cl^-]$ (0.9 g, 2.4 mmol) was added. Concentrated hydrochloric acid was slowly added until no further green solid precipitated. Extraction of the slurry with dichloromethane yielded an emerald green solution, which was separated and dried over anhydrous magnesium sulfate. Concentration in vacuo was followed by the slow addition of carbon tetrachloride. Dark red crystals of $[Ph_4P^+]_2[O_2RuCl_4^{2-}]$ (0.72 g, 0.76 mmol) precipitated upon cooling to −20 °C. IR (KBr): 3058 (w), 1584 (m), 1484 (m), 1437 (s), 1269 (m), 1109 (vs), 997 (m), 828 (s), 762 (m), 756 (m), 722 (vs), 691 (s), 528 (vs) cm^{-1}. UV–vis (CH_2Cl_2) [λ_{max}, nm (ϵ, M^{-1} cm^{-1})]: 261 (7000), 269 (7300), 276 (6000), 353 (2820), 648 (470).

$[PPN^+]_2[O_2RuCl_4^{2-}]$. The ruthenate solution (prepared from 1.2 mmol of RuO_2) was cooled to 0 °C, and a saturated solution of $(Ph_3P)_2N^+Cl^-$ (0.69 g, 1.2 mmol) in water (~200 mL) was slowly added. Neutralization with concentrated hydrochloric acid yielded a green solid, which was extracted with dichloromethane. Workup as described above yielded 0.55 g (0.41 mmol) of $[PPN^+]_2[O_2RuCl_4^{2-}]$. IR (KBr): 3055 (w), 1481 (m), 1437 (s), 1250 (vs), 1112 (s), 997 (m), 834 (m), 803 (w), 750 (m), 722 (vs), 691 (vs), 553 (s), 531 (vs), 497 (vs) cm^{-1}. UV–vis (CH_2Cl_2) [λ_{max}, nm (ϵ, M^{-1} cm^{-1})]: 261 (7000), 269 (7300), 276 (6000), 353 (2820), 648 (470). UV–vis (SiO_2): λ_{max} ~520 nm (arbitrary).

$[Ph_4P^+][O_2RuCl_3^-]$ was prepared according to Griffith's procedure.[4] The magnetic susceptibility was measured in acetonitrile-d_3 with internal and external TMS by using the Evans method[42] and found to be diamagnetic.[30]

$[PPN^+][O_2RuCl_3^-]$. A solution of silver tetrafluoroborate (0.05 mmol) in 1 mL of acetonitrile was added via a Teflon cannula to a solution of $[PPN^+]_2[O_2RuCl_4^{2-}]$ (67.6 mg, 0.05 mmol) in 4 mL of acetonitrile. The resulting precipitate was quickly removed and the solution concentrated in vacuo. Carbon tetrachloride was added slowly to precipitate most of the $[PPN^+][BF_4^-]$. The clear green solution was left in a freezer at −20 °C to yield a mixture of crystals of $[PPN^+][O_2RuCl_3^-]$ and $[PPN^+][BF_4^-]$. Alternatively, a small amount of ruthenium tetraoxide was reduced with aqueous HCl. Addition of a 1-equiv amount of $[PPN^+][Cl^-]$ yielded a green precipitate. Crystallization from a mixture of dichloromethane–carbon tetrachloride yielded emerald green crystals of $[PPN^+][O_2RuCl_3^-]$. IR (KBr): 3058 (w), 1481 (m), 1437 (s), 1262 (s), 1115 (s), 997 (m), 881 (s), 800 (w), 747 (m), 725 (vs), 691 (vs), 550 (vs), 534 (vs), 497 (s) cm^{-1}. UV–vis (CH_2Cl_2) [λ_{max}, nm (ϵ, M^{-1} cm^{-1})]: 261 (7000), 269 (7300), 276 (6000), 353 (2820), 648 (470). UV–vis (SiO_2): λ_{max} ~650 nm (arbitrary).

$[Et_4N^+][O_2RuCl_3^-]$. A solution of ruthenium tetraoxide (1.2 mmol) in carbon tetrachloride was shaken with 8 mL of 3 M hydrochloric acid to effect reduction to a dark red solution of ruthenium(VI). Tetraethylammonium chloride (0.26 g, 1.4 mmol) was added and the resulting solution extracted with dichloromethane. The emerald green solution was dried over anhydrous $MgSO_4$ and concentrated in vacuo. Carbon tetrachloride was slowly added and the solution cooled to −20 °C to produce a shiny flaky solid of $[O_2RuCl_3^-][Et_4N^+]$ (0.06 g, 0.14 mmol). IR (KBr): 2984 (m), 1484 (m), 1456 (m), 1437 (m), 1394 (m), 1172 (m), 1003 (m), 881 (vs), 828 (w), 787 (m) cm^{-1}. UV–vis (CH_2Cl_2) [λ_{max}, nm (ϵ, M^{-1} cm^{-1})]: 261 (7000), 269 (7300), 276 (6000), 353 (2820), 648 (470).

$[n\text{-}Bu_4N^+][O_2RuCl_3^-]$. A solution of ruthenium tetraoxide as above was treated with 1 equiv of tetra-*n*-butylammonium chloride (0.33 g, 1.2 mmol). The green precipitate was also treated similarly to yield $[O_2RuCl_3^-][n\text{-}Bu_4N^+]$ as tiny green flakes. Yield: 0.16 g. IR (KBr): 2966 (vs), 2938 (m), 2875 (s), 1472 (s), 1384 (m), 1169 (w), 1066 (w), 1031 (w), 925 (w), 884 (vs), 800 (w), 737 (w) cm^{-1}. UV–vis (CH_2Cl_2) [λ_{max}, nm (ϵ, M^{-1} cm^{-1})]: 261 (7000), 269 (7300), 276 (6000), 353 (2820), 648 (470).

Instrumentation. Electronic absorption spectra were recorded on a Hewlett-Packard 8450A diode array spectrometer with 2-nm resolution. Infrared spectra were obtained on a Nicolet 10 DX-FT spectrometer with 2–4-cm^{-1} resolution using either KBr disks or Nujol mulls for solid-state measurements and 0.1-mm NaCl cells for solutions. Gas chromatographic analyses were performed on a Hewlett-Packard 5890 chromatograph with a 12.5-m cross-linked dimethylsilicone capillary column. GC–MS measurements were carried out on a Hewlett-Packard 5890 A chromatograph interfaced to a HP 5970 mass spectrometer (EI) operating at 70 eV. Diffuse-reflectance spectra were obtained with a Hitachi integrating sphere (60-mm diameter) attached to a Perkin-Elmer 330 UV–vis spectrometer. ^1H NMR spectra were recorded in chloroform-*d* on a JEOL FX90Q FT spectrometer using TMS as an internal standard.

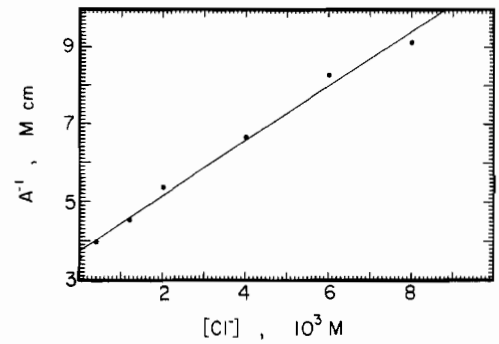

Figure 7. Determination of the formation constant of 6×10^{-4} M $O_2RuCl_4^{2-}$ in dichloromethane by the change in absorbance (A) with incremental additions of $[Et_4N^+][Cl^-]$.

Association Constant for Chloride Anation to Dioxotrichlororuthenate(VI). In a typical experiment, a 5-mL solution of 6×10^{-4} M $[PPh_4^+][O_2RuCl_3^-]$ in dichloromethane was contained in a 1.0-cm cuvette and treated with successive aliquots of 2 M tetraethylammonium chloride in the same solvent. The absorption band at λ_{max} 353 nm for the anionic $O_2RuCl_3^-$ experienced a slight red shift to 357 nm with a slight enhancement in absorbance. More importantly, the change in color of the solution from green to orange resulted from the disappearance of the band at λ_{max} 648 nm and a concomitant increase in the absorbance at ~500 nm. The extinction coefficient of the latter band was determined when the absorbance (A) did not change upon incremental additions of chloride (~40 equiv). The formation constant (K^{-1}) for $O_2RuCl_4^{2-}$ was determined by following the decay of the 648-nm band. The plot of $[Cl^-]$ versus A^{-1} afforded a straight line with a slope given by $K^{-1}[O_2RuCl_3^-]^{-1}\epsilon_{643}^{-1}$ and an intercept given by $[O_2RuCl_3^-]^{-1}\epsilon_{648}^{-1}$, as shown in Figure 7. The formation constant of 1.9×10^2 M^{-1} for $O_2RuCl_4^{2-}$ is equivalent to the dissociation constant $K = 5.3 \times 10^{-3}$ M for chloride loss from $O_2RuCl_4^{2-}$.

X-ray Crystallography of Dioxochlororuthenium(VI) Salts. Dioxotetrachlororuthenate(VI). The structure of $O_2RuCl_4^{2-}$ was determined as the $(Ph_3P)_2N^+$ salt, a single crystal of which was grown by carefully adding 8 mL of benzene as a separate layer onto a solution of 8 mg of $[(Ph_3P)_2N^+]_2[O_2RuCl_4^{2-}]$ in 5 mL of dichloromethane. Partial diffusion at room temperature occurred over a 36-h period to produce dark red orange crystals. A small, crystalline parallelepiped having the approximate dimensions of $0.40 \times 0.40 \times 0.10$ mm was mounted on a glass fiber in random orientation on a Nicolet R3m/V automatic diffractometer. The radiation used was Mo Kα monochromatized by a highly ordered graphite crystal. Final cell constants, as well as other information pertinent to data collection and refinement, are listed in Table III. The Laue symmetry was determined to be $\bar{1}$, and the space group was shown to be either $P1$ or $P\bar{1}$. Intensities were measured by using the θ–2θ scan technique, with the scan rate depending on the count obtained in rapid prescans of each reflection. Two standard reflections were monitored after every 2 h or every 100 data collected, and these showed slow, linear decay amounting to about 15% over the entire course of the data collection. A normalizing factor as a function of exposure time was used to account for this. In reduction of the data, Lorentz and polarization corrections were applied; however, no correction for absorption was made due to the small absorption coefficient. Space group $P\bar{1}$ was assumed from the outset, and the structure was solved by merely placing Ru at the origin. All remaining non-hydrogen atoms were located in subsequent difference Fourier syntheses. The asymmetric unit consists of one complete cation and one-half of an anion on an inversion center. The usual sequence of isotropic and anisotropic refinement was followed, after which all hydrogens were entered in ideal calculated positions and constrained to riding motion. A single variable isotropic thermal parameter was assigned to all of the hydrogen atoms. At this point, a diffuse area of residual electron density was noted about 0, $^1/_2$, $^1/_2$, which was assumed to represent disordered solvent molecules. Eventually six refinable atom positions were located, each being assigned as carbon with 50% occupancy (C(37)–C(42)). Unfortunately, the close proximity of these

(42) Evans, D. F. *J. Chem. Soc.* **1959**, 2003.

Table III. Crystal Data Collection and Processing Parameters[a]

A. $[(Ph_3P)_2N^+]_2[O_2RuCl_4^{2-}]$

chem formula: $(C_{26}H_{30}NP_2^+)_2RuCl_4O_2^-$	fw: 1352[b]
	space group: $P\bar{1}$ (triclinic)
a = 10.916 (2) Å	ρ = 1.26[b] g cm^{-3}
b = 12.378 (2) Å	μ = 4.95[b] cm^{-1}
c = 13.788 (2) Å	R = 0.051
α, β, γ = 105.65 (1), 93.16 (1), 92.60 (1)°	R_w = 0.052
V = 1788 Å^3	
Z = 1	

B. $[(Ph_3P)_2N^+][O_2RuCl_3^-]$

chem formula: $C_{36}H_{30}NP_2^+RuCl_3O_2^-$	fw: 3445
	space group: $P2_1/n$ (monoclinic)
a = 10.629 (4) Å	ρ = 1.50 g cm^{-3}
b = 15.636 (5) Å	μ = 8.04 cm^{-1}
c = 21.026 (7) Å	R = 0.032
β = 99.60 (2)°	R_w = 0.022
V = 3445 Å^3	
Z = 4	

C. $[Ph_4P^+][O_2RuCl_3^-]$

chem formula: $C_{24}H_{20}P^+RuCl_3O_2^-$	fw: 1251
	space group: $P4/n$ (tetragonal)
a = 12.672 (2) Å	ρ = 1.54 g cm^{-3}
c = 7.788 (2) Å	μ = 10.2 cm^{-1}
V = 1251 Å^3	R = 0.042
Z = 2	R_w = 0.024

[a] Radiation (Mo Kα) λ = 0.71073 Å; T = 25 °C; weights $w = \sigma(F)^{-2}$; $R = \sum||F_o| - |F_c||/\sum|F_o|$; $R_w = [\sum w(|F_o| - |F_c|)^2/\sum w|F_o|^2]^{1/2}$. [b] Excludes solvent.

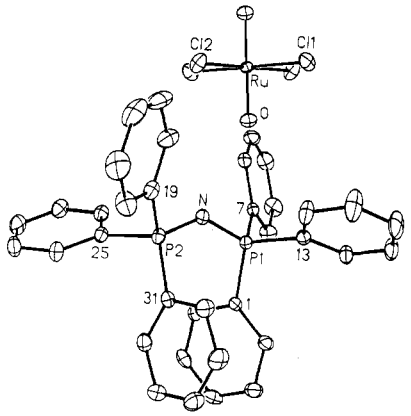

Figure 8. ORTEP diagram of $[(Ph_3P)_2N^+][O_2RuCl_4^{2-}]$, showing the atom-labeling scheme.

positions rules out any molecular assignments based on the known solvents that were introduced during the course of the synthesis and recrystallizations. It is possible that C(37)–C(39) and their inversion relatives represent benzene, and thus these three atoms were refined as a rigid group. The remaining disordered atoms may be other partial benzene sites or may be due to several lone water molecules. In fact, it is possible that all six solvent positions may be waters having various occupancies ranging from 25% to 40%. After all shift/esd ratios were less than 0.2 (except for C(37)–C(42)), convergence was reached at the agreement factors listed in Table IV. No unusually high correlations were noted between any of the variables in the last cycle of full-matrix least-squares refinement, and the final difference density map showed no peaks greater than 0.50 e/Å^3. All calculations were made by using Nicolet's SHELXTL PLUS series of crystallographic programs.[33]

Dioxotrichlororuthenate(VI). The structures of $O_2RuCl_3^-$ were determined as both the $(Ph_3P)_2N^+$ and the Ph_4P^+ salts as follows.

A single crystal of $[(Ph_3P)_2N^+][O_2RuCl_3^-]$ was obtained from the admixture of the salts (vide supra) by dissolving 10 mg of the crystals in 1 mL of dichloromethane and adding 3 mL of carbon tetrachloride. The solution was cooled to −20 °C in a freezer and yielded a diamond-shaped emerald green crystal of $[(Ph_3P)_2N^+][O_2RuCl_3^-]$ among others. A thick irregular slab having approximate dimensions 0.50 × 0.35 × 0.20 mm was carved from the center of the diamond-shaped plate and mounted in a random orientation on the diffractometer (vide supra). The final cell constants, as well as other information pertinent to data collection and refinement, are listed in Table III. The Laue symmetry was

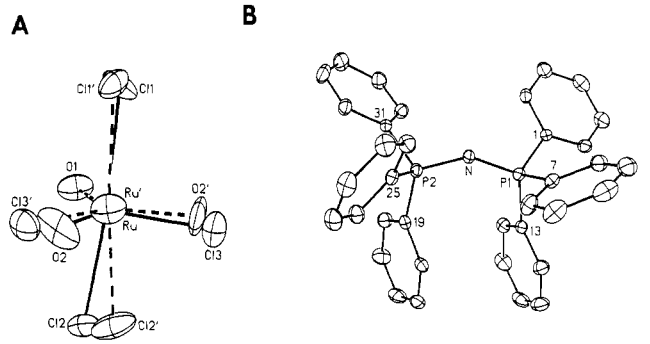

Figure 9. ORTEP diagrams of (A) the disorder in the $O_2RuCl_3^-$ structure and (B) the $(Ph_3P)_2N^+$ structure as described in the text.

determined to be $2/m$, and from the systematic absences noted, the space group was shown unambiguously to be $P2_1/n$. Intensities were measured by using the ω scan technique, as described above. The structure was solved by use of the SHELXTL Patterson interpretation program,[33] which revealed the position of the Ru atom in the anion. The remaining non-hydrogen atoms were located in subsequent difference Fourier syntheses. The hydrogen atoms were added at ideal calculated positions and constrained to riding motion, with nonvariable isotropic thermal parameters. It was quickly found that the anion was disordered over two slightly different positions, such that one of the equatorial oxygen sites was exchanged with the chlorine site essentially 50% of the time. When this model was refined, it was noted that the equatorial planes of the two orientations were tipped at about 8° to each other, and the axial Cl atoms displayed very high "thermal motion". Therefore, a new model was assumed in which the Ru sites of the two orientations were not coincident. Unfortunately, since the atoms involved were quite close to each other, some very high correlations appeared in the least squares. In order to minimize the effect of this proximity, the bond distances involving the offending atoms were constrained to be roughly equal to freely refined variable values. Three separate parameters were used, corresponding to Ru–Cl(ax), Ru–Cl(eq), and Ru–O(eq). This model refined so well that anisotropic thermal motion could be introduced. The O(1) and O(1′) atoms were found to be essentially coincident, and thus O(1′) was abandoned and O(1) refined at 100% occupancy. All other atoms in the two separate orientations were given 50% occupancy, on the basis of the examination of the thermal motion at equivalent sites (see Figure 9A). By contrast, the cationic $(Ph_3P)_2N^+$ refined without disorder (see Figure 9B). After all shift/esd ratios were less than 1.0, convergence was reached at the agreement factors listed in Table IV. No unusually high correlations were noted between any of the variables in the last cycle of the full-matrix least-squares refinement (except those of the closely paired disordered sites in the anion), and the final difference density map showed no peak greater than 0.2 e/Å^3.

A single crystal of $[Ph_4P^+][O_2RuCl_3^-]$ was grown from 6 mg of salt dissolved in 1 mL of dichloromethane by allowing the vapor diffusion of *n*-pentane at −20 °C for 4 days. A very small, dark emerald green square-columnar crystal having approximate dimensions 0.44 × 0.08 × 0.08 nm was mounted in a random orientation on the diffractometer (vide supra). The final cell constants, as well as other information pertinent to data collection and refinement, are listed in Table III. The Laue symmetry was determined to be $4/m$, and from the systematic absences noted, the space group was shown unambiguously to be $P4/n$. Intensities were measured using the ω scan technique as described above. The structure was solved by use of the SHELXTL PLUS Patterson interpretation program.[33] It revealed the position of the Ru atom in the asymmetric unit, which consists of one-quarter anion lying on a 4-fold axis and one-quarter of the cation lying on a $\bar{4}$ symmetry site. The remaining non-hydrogen atoms were located in subsequent difference Fourier syntheses. Hydrogens were added at ideal calculated positions and constrained to riding motion, with nonvariable isotropic thermal parameters. It was quickly found that the anion was massively disordered over at least eight different positions. In fact, there appeared to be two different geometric isomers involved. When given full occupancy, the chlorine atoms displayed very large thermal parameters, and since there were four symmetry-equivalent sites and only three atoms per anion, the population was reset to 75% and held fixed. At first it appeared as if the correct model would be a square pyramid (sp) having two trans equatorial oxo bonds that were disordered over four positions such that the Ru–O bonds were coincident with the 4-fold axis. However, the temperature factor of O(2) was very large and that of O(1) was considerably larger than expected on the basis of observation of the Cl atom. Also, a very small peak appeared in the electron density map in the vicinity of O(2). This knowledge together with the trigonal-bipyramidal (tbp)

Table IV. Atomic Coordinates ($\times 10^4$) and Equivalent Isotropic Displacement Parameters ($Å^2 \times 10^3$) for Dioxochlororuthenium(VI) Complexes

	x	y	z	$U(eq)^a$		x	y	z	$U(eq)^a$
				A. $[(Ph_3P)_2N^+]_2[O_2RuCl_4^{2-}]$					
Ru	0	0	0	36 (1)	C(19)	5925 (6)	7260 (5)	4680 (5)	47 (2)
Cl(1)	−1160 (2)	1451 (1)	966 (2)	70 (1)	C(20)	5155 (7)	6617 (6)	5096 (5)	64 (3)
Cl(2)	1761 (2)	670 (1)	1157 (1)	69 (1)	C(21)	5310 (10)	6717 (7)	6117 (6)	89 (4)
P(1)	3427 (1)	6808 (1)	2138 (1)	33 (1)	C(22)	6192 (11)	7455 (9)	6708 (6)	98 (5)
P(2)	5789 (1)	7062 (1)	3336 (1)	36 (1)	C(23)	6939 (9)	8090 (9)	6309 (6)	96 (5)
O	457 (4)	896 (3)	−680 (3)	55 (2)	C(24)	6817 (7)	7982 (7)	5303 (5)	72 (3)
N	4434 (4)	6573 (4)	2917 (3)	39 (2)	C(25)	6887 (5)	6055 (5)	2813 (4)	39 (2)
C(1)	4052 (5)	7338 (4)	1178 (4)	34 (2)	C(26)	8132 (6)	6304 (5)	3029 (5)	53 (3)
C(2)	3760 (6)	8352 (5)	1000 (5)	47 (2)	C(27)	8951 (6)	5497 (6)	2674 (5)	64 (3)
C(3)	4324 (7)	8723 (6)	247 (5)	61 (3)	C(28)	8515 (7)	4432 (6)	2112 (5)	63 (3)
C(4)	5173 (7)	8100 (6)	−299 (5)	62 (3)	C(29)	7301 (7)	4186 (5)	1908 (5)	55 (3)
C(5)	5461 (6)	7081 (6)	−132 (5)	56 (3)	C(30)	6477 (6)	4987 (5)	2241 (4)	43 (2)
C(6)	4901 (5)	6696 (5)	593 (4)	42 (2)	C(31)	6212 (5)	8384 (5)	3118 (4)	38 (2)
C(7)	2585 (5)	5508 (4)	1522 (4)	36 (2)	C(32)	6941 (6)	8469 (5)	2330 (5)	50 (3)
C(8)	2089 (6)	5297 (5)	539 (5)	51 (3)	C(33)	7132 (7)	9484 (6)	2103 (6)	65 (3)
C(9)	1417 (6)	4289 (6)	89 (5)	64 (3)	C(34)	6596 (7)	10422 (6)	2667 (7)	72 (4)
C(10)	1220 (7)	3500 (6)	605 (6)	64 (3)	C(35)	5881 (7)	10347 (6)	3439 (6)	70 (3)
C(11)	1688 (6)	3719 (5)	1583 (6)	60 (3)	C(36)	5698 (6)	9345 (5)	3662 (5)	55 (3)
C(12)	2382 (5)	4706 (5)	2046 (5)	46 (2)	C(37)	−130 (16)	3623 (13)	4406 (13)	100
C(13)	2337 (5)	7741 (5)	2769 (4)	39 (2)	C(38)	949	4278	4484	100
C(14)	2459 (7)	8165 (6)	3812 (5)	66 (3)	C(39)	1023	5396	5008	100
C(15)	1600 (8)	8844 (8)	4314 (6)	101 (4)	C(40)	1913 (18)	6787 (17)	5809 (15)	104 (6)
C(16)	635 (8)	9130 (7)	3785 (6)	91 (4)	C(41)	1864 (19)	5951 (18)	5254 (16)	108 (7)
C(17)	503 (7)	8724 (6)	2755 (6)	70 (3)	C(42)	33 (24)	2586 (22)	4123 (20)	127 (9)
C(18)	1342 (6)	8034 (5)	2250 (5)	51 (3)					
				B. $[(Ph_3P)_2N^+][O_2RuCl_3^-]$					
Ru	965 (3)	905 (2)	3041 (1)	42 (1)	C(12)	4585 (4)	2607 (3)	1808 (2)	53 (2)
Ru′	942 (4)	933 (3)	3065 (2)	93 (2)	C(13)	7441 (3)	3299 (2)	1026 (2)	37 (2)
Cl(1)	−231 (10)	2188 (5)	2841 (5)	92 (4)	C(14)	7893 (4)	3619 (3)	492 (2)	46 (2)
Cl(1′)	−331 (9)	2151 (5)	2808 (4)	74 (3)	C(15)	8889 (4)	4195 (3)	575 (3)	64 (2)
Cl(2)	2099 (10)	−421 (5)	3138 (4)	78 (2)	C(16)	9412 (5)	4457 (3)	1186 (3)	73 (2)
Cl(2′)	2304 (9)	−219 (5)	3382 (4)	116 (4)	C(17)	8963 (5)	4163 (3)	1710 (3)	69 (2)
Cl(3)	2347 (4)	1446 (3)	3784 (2)	97 (2)	C(18)	7967 (4)	3578 (3)	1638 (2)	54 (2)
Cl(3′)	−793 (5)	190 (4)	3056 (3)	71 (2)	C(19)	9166 (3)	1631 (2)	458 (2)	37 (2)
P(2)	7672 (1)	1084 (1)	406 (1)	36 (1)	C(20)	9759 (4)	1932 (3)	1052 (2)	43 (2)
P(1)	6185 (1)	2514 (1)	880 (1)	35 (1)	C(21)	10850 (4)	2432 (3)	1099 (2)	53 (2)
O(1)	1415 (3)	1013 (2)	2327 (2)	87 (2)	C(22)	11347 (4)	2619 (3)	548 (3)	65 (2)
O(2)	−324 (12)	365 (10)	3207 (9)	107 (7)	C(23)	10777 (4)	2303 (3)	−40 (3)	68 (2)
O(2′)	1453 (9)	1394 (7)	3832 (4)	96 (4)	C(24)	9690 (4)	1814 (3)	−84 (2)	53 (2)
N	6552 (3)	1673 (2)	545 (2)	40 (1)	C(25)	7909 (4)	186 (2)	943 (2)	38 (2)
C(1)	4932 (3)	3037 (3)	347 (2)	35 (2)	C(26)	6853 (4)	−211 (3)	1118 (2)	52 (2)
C(2)	4596 (4)	3866 (3)	477 (2)	47 (2)	C(27)	7001 (5)	−923 (3)	1501 (2)	64 (2)
C(3)	3690 (4)	4296 (3)	47 (2)	60 (2)	C(28)	8205 (5)	−1235 (3)	1725 (2)	65 (2)
C(4)	3163 (4)	3909 (3)	−517 (2)	63 (2)	C(29)	9262 (5)	−840 (3)	1564 (2)	60 (2)
C(5)	3488 (4)	3091 (3)	−656 (2)	59 (2)	C(30)	9123 (4)	−130 (3)	1166 (2)	49 (2)
C(6)	4365 (4)	2646 (3)	−218 (2)	45 (2)	C(31)	7249 (3)	669 (2)	−394 (2)	36 (2)
C(7)	5673 (4)	2265 (2)	1632 (2)	39 (2)	C(32)	6803 (4)	1222 (3)	−897 (2)	49 (2)
C(8)	6392 (5)	1683 (3)	2040 (2)	58 (2)	C(33)	6536 (4)	931 (3)	−1522 (2)	61 (2)
C(9)	6020 (6)	1449 (3)	2615 (2)	72 (2)	C(34)	6675 (5)	77 (3)	−1648 (2)	70 (2)
C(10)	4923 (6)	1778 (3)	2775 (3)	76 (3)	C(35)	7082 (5)	−479 (3)	−1154 (3)	70 (2)
C(11)	4202 (5)	2356 (3)	2385 (3)	71 (2)	C(36)	7383 (4)	−193 (3)	−528 (2)	52 (2)
				C. $[Ph_4P^+][O_2RuCl_3^-]$					
Ru	2500	2500	1753 (1)	71 (1)	C(1)	1379 (4)	7383 (5)	1376 (6)	43 (2)
Cl	890 (2)	1556 (2)	1898 (3)	100 (1)	C(2)	1293 (4)	8043 (5)	2807 (6)	59 (3)
P	2500	7500	0	43 (1)	C(3)	464 (6)	7933 (6)	3923 (8)	76 (3)
O(1)	2500	2500	−539 (41)	49 (9)	C(4)	−283 (6)	7173 (6)	3655 (9)	89 (4)
O(1′)	2863 (39)	2716 (56)	−176 (31)	50 (11)	C(5)	−219 (5)	6541 (6)	2235 (9)	89 (3)
O(2)	2500	2500	3871 (31)	82 (9)	C(6)	617 (5)	6619 (5)	1094 (7)	62 (3)
O(2′)	3125 (23)	2870 (26)	3502 (30)	71 (9)					

[a] Equivalent isotropic U defined as one-third of the trace of the orthogonalized U_{ij} tensor.

structure of the PPN^+ salt (vide supra) suggested that both geometries were present, each disordered such that their three Cl atoms occupied essentially the same sites about the 4-fold axis. Additionally, both must be disordered over four different positions. In order for this model to be valid, there must be another O site roughly 120° from Cl and O(2′), although it would only be present 15% of the time. Thus, it was not surprising it could not be found in the difference map. An approximately positioned O(1′) was added, and it freely refined as well as O(2′). This refinement lent credence to the proposed model. Initially, this model was refined as if both geometries were present in equal amounts; however, analysis of the isotropic temperature factors of the oxygens led to the conclusion that the correct ratio was actually closer to a 60:40 ratio of the tbp and sp forms, respectively. Thus, in the final refinement, the following occupancies were used: Ru, 0.25; Cl, 0.75; O(1) and O(2), 0.10; O(1′) and O(2′), 0.15. These resulted in the correct 60:40 ratio when the 4-fold axis was taken into account. Since $R = 0.042$ was obtained in the final refinement, with essentially no residual electron density above background, the positioning of the electron density in the asymmetric unit was essentially correct. However, from an examination of the composite structure in Figure 10A showing the complete 4-fold disordered symmetry, many possible molecular geometries can be proposed by connecting differing atomic sites. If reasonable geometric constraints were applied, such as insisting that each anion contain three Cl and two O atoms with no angles less than 80° or greater than 140°, the combined tbp/sp model given above appeared most plausible. With such extensive disorder, however, it was impossible to rule out with

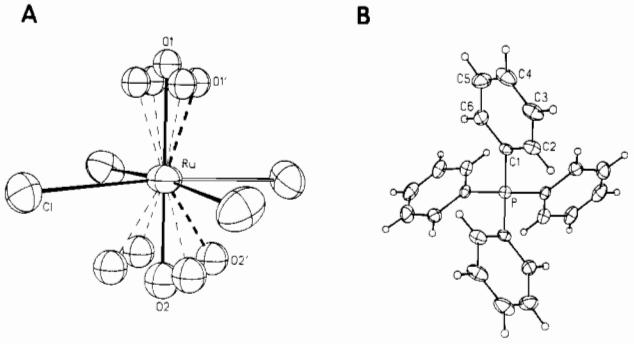

Figure 10. ORTEP diagrams of (A) the disorder in the $O_2RuCl_3^-$ structure and (B) the Ph_4P^+ structure as described in the text.

certainty any of the more exotic interpretations. The ORTEP diagram of the cationic Ph_4P^+ structure is shown in Figure 10B. After all shift/esd ratios were less than 0.1, convergence was reached at the agreement factors listed in Table IV. No unusually high correlations were noted between any of the variables in the last cycle of full-matrix least-squares refinement, and the final difference density map showed no peak greater than 0.3 e/Å^3.

Oxygen Atom Transfer from Dioxochlororuthenium(VI). Owing to the extensive dissociation of $O_2RuCl_4^{2-}$ according to eq 1, in solution the active oxidant is $O_2RuCl_3^-$ irrespective of the dioxochlororuthenium(VI) salt employed.

Phosphine Donors. Typically, a solution of $[Ph_4P^+][O_2RuCl_3^-]$ (57.8 mg, 0.10 mmol) in 5 mL of acetonitrile was treated with triphenylphosphine (26.2 mg, 0.10 mmol). After the solution was stirred for 3 h, it turned green black. It was concentrated by the removal of the solvent in vacuo, and 10 mL of diethyl ether was added. The dark green solid (52 mg) was collected, and quantitative analysis of the colorless filtrate by GC–MS indicated the presence of 0.10 mmol of free triphenylphosphine oxide by the internal standard method. Removal of the solvent yielded 24 mg of the colorless solid. Similarly, the treatment of $[Ph_4P^+][O_2RuCl_3^-]$ (28.9 mg, 0.05 mmol) in 4 mL of dichloromethane with dimethylphenylphosphine (0.05 mmol) was carried out under an argon atmosphere for 1 h. Workup as described above yielded 35 mg of a dark green solid. GC analysis of the colorless filtrate did not show evidence of free dimethylphenylphosphine oxide. However, when the dark green solid that showed an IR band at 1131 cm^{-1} was treated with pyridine, $OPMe_2Ph$ was liberated.

Cyclohexene. A solution of $[Ph_4P^+][O_2RuCl_3^-]$ (28.9 mg, 0.05 mmol) in 1 mL of either acetonitrile or dichloromethane was treated with 0.05 mmol of cyclohexene and 0.009 mmol of *n*-decane as the internal standard. In both solvents a dark green solid precipitated over the course of several hours. Diethyl ether (2 mL) was added to ensure complete separation of the reduced ruthenium species. GC–MS analysis of the colorless supernatant liquid was as follows for reactions carried out in acetonitrile (dichloromethane) [$\times 10^{-3}$ mmol]: cyclohexene oxide, 2 (0); 2-cyclohexenone, 3 (3); 2-chlorocyclohexanone, 3 (6); 2-chlorocyclohexanol, 2 (4). The cyclohexene consumed was 12 (16) $\times$ 10^{-3} mmol for 95% (95%) material balance. The retention times on a 12.5-m cross-linked dimethylsilicone capillary column at 40 °C for 0.5 min and programmed at 10 °C min^{-1} were as follows: cyclohexene, 1.01; cyclohexene oxide, 2.47; 2-cyclohexenone, 3.26; 2-chlorocyclohexanol, 4.76; 2-chlorocyclohexanone, 4.98. Mass spectral cracking patterns [*m*/*z* (%)] were as follows. 2-Chlorocyclohexanol: 98 (8), 87 (11), 81 (17), 80 (24), 57 (100), 55 (9), 44 (21), 43 (13), 42 (12), 41 (13). 2-Chlorocyclohexanone: 132 (21), 97 (22), 90 (8), 88 (25), 70 (9), 69 (18), 68 (22), 55 (100). The mass spectra of cyclohexene oxide and cyclohexenone were compared with authentic standards.

Phenol. A solution of $[Ph_4P^+][O_2RuCl_3^-]$ (29 mg, 0.05 mmol) in 2 mL of acetonitrile was treated with 2,6-di-*tert*-butylphenol (31 mg, 0.15 mmol). The color changed to green-black on mixing. After 2 h, the solvent was mostly removed in vacuo, and 3 mL of diethyl ether was added. Qualitative analysis of the orange filtrate indicated the presence of 2,6-di-*tert*-butyl-1,4-benzoquinone and 3,5,3′,5′-tetra-*tert*-butyldiphenoquinone [^{1}H NMR ($CDCl_3$): δ 7.70 (s, 1 H), 1.36 (s, 9 H)].[40,41]

Acknowledgment. We thank the National Science Foundation and the R. A. Welch Foundation for financial support, J. D. Korp for crystallographic assistance, and T. C. Lau for many helpful discussions and the initial studies that elucidated the products of cyclohexene oxidation.

Supplementary Material Available: For the dioxochlororuthenate(VI) salts, tables of complete crystal data collection and processing parameters, anisotropic thermal parameters, and complete bond lengths and angles (8 pages); listings of observed and calculated structure factors (28 pages). Ordering information is given on any current masthead page.